Steady State Multiplicity and Partial Internal Wetting of Catalyst Particles

The partial internal wetting of spherical catalyst particles exposed to saturated vapor is investigated here by considering the interplay of capillary condensation phenomena and thermal effects for a first-order irreversible reaction. It is shown that for certain very narrow ranges of parameters steady states can exist in which the macropores are vapor-filled while micropores in an inner core, or an outer shell, are liquid-filled. Under certain conditions even two such steady states are found, although only one of them can be stable. In addition to these there exist states in which all the micropores are liquid-filled or those in which the entire particle is internally dry.

S. K. Bhatia
Department of Chemical Engineering
Indian Institute of Technology
Powai, Bombay 400 076, India

Introduction

The incomplete wetting of catalyst particles is a problem of immediate concern in trickle-bed reactor operation, and has received considerable attention in recent years. Experimental evidence (Sedriks and Kenney, 1973; Satterfield and Ozel, 1973; Hanika et al., 1976; Colombo et al., 1976; Herskowitz et al., 1979) appears to indicate that the degree of external wetting can lie anywhere between 0 and 100%, corresponding to completely dry and completely wet particles. For particles completely dry externally, Sedriks and Kenney and Hanika et al. deduce the absence of internal wetting from the interpretations of their experimental data, while in contrast Satterfield and Ozel find visual evidence of internal wetting for such particles. Support for the internal wetting of externally dry particles is also available in the work of Colombo et al. Thus, it would appear that there are at least two steady states for a catalyst particle exposed to a saturated vapor. Nevertheless, most analyses of the effect of external wetting (Ramachandran and Smith, 1979; Mills and Dudukovic, 1980, 1982; Herskowitz, 1981a,b; Yentekakis and Vayenas, 1987) have assumed completely liquid-filled pores regardless of the external environment. In addition, all of these studies have assumed negligible internal and external temperature gradients, so that thermal effects are not addressed.

In other work (Kim and Kim, 1981a) controlled experiments with the hydrogenation of cyclohexene using only a few particles at a time have demonstrated the existence not only of the liquid-filled and vapor-filled states, for particles exposed to saturated gas, but also the presence of at least two other intermediate states corresponding to incomplete internal wetting. One of these was quantitatively simulated (Kim and Kim, 1981b) by assuming that the micropores were completely liquid-filled, while the macropores were vapor-filled. The other steady state was not explained theoretically. Attempts by the authors by considering the micropores to be only partially liquid-filled were not successful. An additional speculation of Kim and Kim that this state may correspond to a situation in which one of the two catalyst pellets used was in the vapor-filled state while the other was in the micropore liquid-filled state does not seem plausible because the state was stable over a wide range of hydrogen partial pressures.

A factor not directly addressed by the models of Kim and Kim and all other prior investigators is the interplay of capillary condensation phenomena and thermal effects in determining the steady state behavior. The cyclohexene-hydrogen reaction is zero order in cyclohexene and of order 0.5 to 1 in hydrogen. In this work we consider the even simpler case of an irreversible first-order reaction of a saturated gas according to $A \rightarrow B$ and demonstrate that capillary condensation phenomena and thermal effects can combine to yield other steady states in which micropores in an inner core, or an external shell, are liquid-filled while the rest of the particle is vapor-filled. It may be mentioned here that partial internal wetting has also been considered by Sakornwimon and Sylvester (1982), but capillary condensation phenomena and thermal effects were ignored. As a result the multiple steady states were not predicted. In other work Drobyshevich et al. (1983) also considered the problem of reaction of a condensable vapor with thermal effects, but did not include considerations of capillary condensation, with the result that only unique steady states were predicted. More recently Hu and Ho (1987) have considered the multiplicity arising out of thermal

and diffusional effects in an externally partially wetted, but internally completely liquid-filled, catalyst. However, partial internal wetting related to capillary condensation equilibria was not treated.

Vapor-Liquid and Reaction Equilibria in Cylindrical Pores

If a heterogeneous reaction were to occur in a catalyst particle under conditions of only partial internal wetting, then material transfer would take place at the phase boundaries, with reaction on the pore surfaces. For a single component the equilibrium in a pore is well described by the classical Kelvin equation (Defay and Prigogine, 1966; Gregg and Sing, 1981), while for condensation in an empty cylindrical pore open at both ends Cohan (1938) has derived the result for the necessary pressure. A treatment of the thermodynamics for the multicomponent case, but under nonreacting conditions, has been provided by Everett (1975) and an equation for the phase equilibrium given, albeit without derivation. For the case of reaction, however, there appears little in the literature, and it is pertinent therefore to consider the reaction equilibrium in a pore in the presence of a vapor-liquid interface.

Consider a cylindrical pore having a hemispherical vapor-liquid interface, which is surrounded by an infinite reservoir of vapor, and let a small amount of reaction with net liquid phase extent $\delta\zeta$ occur on the pore surface. The resulting Gibbs free energy change is given by

$$\delta G = \sum_i \epsilon_i \bar{G}_i^l \, \delta\zeta - 2\pi r \sigma \cos\hat{\theta} \, \delta l \tag{1}$$

in which the first term is the usual bulk free energy change, while the second term represents the work related to the interface movement. The movement of the interface arises because of the difference in the partial molar volumes of reactants and products, which are assumed to be miscible. As a result one has

$$\pi r^2 \, \delta l = \sum_i \epsilon_i \bar{v}_i \, \delta\zeta \tag{2}$$

and at equilibrium, whence $\partial G/\partial\zeta = 0$, Eqs. 1 and 2 combine to give

$$\prod_{i=1}^{N} \hat{a}_i^{\epsilon_i} = \exp\left[-\left(\frac{\Delta G^o}{R_g T} - \frac{2\sigma \cos\hat{\theta} \, \Delta v}{r R_g T}\right)\right] \tag{3}$$

in which, as usual, we have written

$$\bar{G}_i^l = G_i^o + R_g T \ln(\hat{a}_i) \tag{4}$$

where G_i^o refers to a standard state at the same temperature, and

$$\Delta G^o = \sum_i \epsilon_i G_i^o \tag{5}$$

$$\Delta v = \sum_i \epsilon_i \bar{v}_i \tag{6}$$

Thus, we see that for the liquid phase the reaction equilibrium constant is modified by a factor $\exp(2\sigma \cos\hat{\theta} \, \Delta v/r R_g T)$ due to the curvature of the pore surface. The same would not be true for the gas phase, which is assumed to be an infinite reservoir, as is the situation arising for an externally dry catalyst particle. Nevertheless, if vapor-liquid equilibrium exists, the reaction rates in the liquid and vapor phases will still be the same because of equality of the species chemical potentials in the two phases (Sedriks and Kenney, 1973). However, the reaction rates at pore surfaces far from the vapor-liquid interface may be lower due to liquid-phase concentration gradients. Accordingly it is pertinent to consider if the effect of curvature on the equilibrium constant is significant. While this depends upon the value of Δv for the reaction, for an approximate order of magnitude calculation we may consider $\Delta v = -0.038$ m^3/kmol, which has the same magnitude as the partial molar volume of hydrogen in a number of organic solvents (Reid et al., 1977), and choose $\sigma \cos\hat{\theta} = 0.01$ J/m^2 and $T = 500$ K. For a micropore diameter of 25 Å, this corresponds to a reduction of 14% in the equilibrium constant. For other values of the parameters the effect may be more or less, but it is clear that it can be significant and merits inclusion in analysis, when applicable.

To derive the conditions for vapor-liquid equilibrium we again consider a cylindrical capillary with a hemispherical meniscus. When a small amount δn_i of component i evaporates, at equilbrium

$$\delta n_i(\bar{G}_i^v - \bar{G}_i^l) + 2\pi r \sigma \cos\hat{\theta} \, \delta l = 0 \tag{7}$$

where

$$\delta n_i = \pi r^2 \, \delta l/\bar{v}_i \tag{8}$$

Following standard treatments (Sandler, 1977) we may write,

$$\bar{G}_i^v - \bar{G}_i^l = R_g T \ln\left(\frac{\hat{f}_i^v}{\hat{f}_i^l}\right) = R_g T \ln\left[\frac{\hat{\phi}_i \, y_i \, P}{x_i \, \phi_i^{sat} \, p_i^o \, \gamma_i (f_i^l/f_i^{sat})}\right] \tag{9}$$

which combines with Eqs. 7 and 8 to yield

$$\frac{y_i P}{x_i P_i^o} = \frac{\phi_i^{sat} \gamma_i}{\hat{\phi}_i}\left(\frac{f_i^l}{f_i^{sat}}\right) \exp(-2\sigma \cos\hat{\theta} \, \bar{v}_i/r R_g T) \tag{10}$$

This is the more general form of the result given by Everett (1975) and the classical Kelvin equation is clearly its one-component specialization. For condensation in an empty pore, following Cohan (1938), Eq. 8 is to be modified to

$$\delta n_i = 2\pi r l \, \delta r/\bar{v}_i \tag{11}$$

and the second term in Eq. 7 obtained instead as $2\pi l \sigma \, \delta r$ since, in the absence of condensate in the pore, a cylindrical meniscus will first form. These modifications result in

$$\frac{y_i P}{x_i P_i^o} = \frac{\phi_i^{sat} \gamma_i}{\hat{\phi}_i}\left(\frac{f_i^l}{f_i^{sat}}\right) \exp(-\sigma \bar{v}_i/r R_g T) \tag{12}$$

for the conditions that will be satisfied when condensation begins in a vapor-filled pore. Once condensation has occurred and a hemispherical meniscus has been formed the equilibrium is specified by Eq. 10. Equations 10 and 12 form the principal relations of capillary vapor-liquid equilibrium that will be useful

in the subsequent analysis, although simplifications will be made.

Model Formulation

Consider an irreversible first-order reaction $A \rightarrow B$ occurring in a spherical catalyst particle under conditions in which the particle is surrounded by a gas phase saturated in A. While admittedly simplistic, the reaction may also be representative of hydrogenation in the presence of a large excess of hydrogen so that the kinetics is effectively first order in A. If the reaction is exothermic the steady state intraparticle temperature will be higher than the ambient value, reducing the tendency for capillary condensation. However, since the surrounding gas is saturated in A a low reaction rate steady state may exist in which condensation has occurred in the entire pore structure and both macropores and micropores are liquid-filled. This state of complete liquid-filling is not of interest to us, and we seek to examine the possibility of steady states in which only the micropores are liquid-filled while all the macropores are vapor-filled. Among these are states in which the conditions for vapor-liquid equilibrium in Eq. 10 are satisfied at some radial position R_c within the particle ($0 \le R_c \le R_o$). When this occurs micropores on one side of this position will be liquid-filled while those on the other side will be vapor-filled. For example, if at the prevailing intraparticle temperature for the steady state $P_B^o > P_A^o$, then micropores in the A-rich region $R_c \le R \le R_o$ will be liquid-filled while those in the region $0 \le R < R_o$ will be vapor-filled. If instead $P_A^o > P_B^o$ at the prevailing temperature, then micropores in the inner core, i.e., in the region $0 \le R \le R_c$, will be liquid-filled while those in the outer A-rich region $R_c < R \le R_o$ will be vapor-filled. With the intention of exploring the possibility of such steady states we formulate the mathematical model under the following assumptions.

1. Mass transfer is controlled by intraparticle diffusion, and external boundary layer concentration differences are negligible
2. Heat transfer is controlled by the external boundary layer resistance, so that internal temperature gradients are negligible
3. Liquid- and vapor-phase micropore Thiele moduli are small, so that the micropore effectiveness factor is unity everywhere
4. The reaction is irreversible and its rate for the vapor phase is first order in the concentration of A
5. Macropores are large enough in radius that no wetting takes place in these pores for the steady states under investigation
6. There is negligible bulk motion in the gas phase
7. Intraparticle transport is dominated by vapor-phase diffusion and radial liquid-phase transport rates are negligible
8. Liquid-phase reaction rate in the micropores is the same as that in the vapor phase in the surrounding macropores
9. Micropore radius is everywhere uniform and equal to r

Among these, assumptions 1, 2, and 3 are well established for catalytic reactions and have found ample justification in the literature (Froment and Bischoff, 1979), while assumptions 4 and 5 have already been discussed above (see also the Appendix). Assumption 6 will be satisfied for the simple $A \rightarrow B$ transformation, because of equimolar counterdiffusion, and for hydrogenation in the presence of a large excess of hydrogen. Assumption 7 may be justified on the grounds that liquid-phase diffusivities are four to five orders of magnitude lower than their gas phase counterparts. Further, capillary transport of liquid may be neglected, for on crossing the radial position $R = R_c$ where equilibrium holds, the vapor-liquid interface will be unstable and spontaneous evaporation will occur. In 8 we have made the tacit assumption that the lack of vapor-liquid equilibrium in the region where micropores are liquid-filled, and macropores are vapor-filled, has negligible influence on the liquid phase reaction rate. As already mentioned, in the presence of thermodynamic equilibrium, the vapor and liquid phase reaction rates must indeed be equal because of the equality of the chemical potentials (Sedriks and Kenney, 1973). The effect of nonequilibrium in the liquid-filled region is therefore not addressed here and consigned for future study. Finally, assumption 10 considerably simplifies numerical calculations.

Under these assumptions, the following mathematical model may now be formulated.

Mass transfer

The catalyst particle is divided into an outer region $\eta_c < \eta \le 1$ with effective diffusivity of A as D_{eA1}, and an inner region $0 \le \eta < \eta_c$ with effective diffusivity D_{eA2}. One of these effective diffusivities will correspond to that obtained when only the macropore structure is available for vapor-phase transport, while the other will correspond to the case when the entire pore structure is available. The mass transfer is then modeled by the dimensionless equations

$$\frac{1}{\eta^2}\frac{d}{d\eta}\left(\frac{\eta^2 dC_{A1}^*}{d\eta}\right) = \phi^2 C_{A1}^* e^{-\epsilon(1-\theta)/\theta},\ \eta_c < \eta \le 1 \tag{13}$$

$$\frac{1}{\eta^2}\frac{d}{d\eta}\left(\eta^2 \frac{dC_{A2}^*}{d\eta}\right) = \frac{\phi^2}{\delta} C_{A2}^* e^{-\epsilon(1-\theta)/\theta},\ 0 \le \eta < \eta_c \tag{14}$$

$$C_{A1}^*(\eta_c) = C_{A2}^*(\eta_c) \tag{15}$$

$$\frac{dC_{A1}^*}{d\eta} = \delta \frac{dC_{A2}^*}{d\eta} \quad \text{at} \quad \eta = \eta_c \tag{16}$$

$$C_{A1}^*(1) = 1 \tag{17}$$

$$\frac{dC_{A2}^*}{d\eta} = 0 \quad \text{at} \quad \eta = 0 \tag{18}$$

Equations 15 and 16 ensure continuity of the concentration of A and of its mass transfer rate, respectively, at $\eta = \eta_c$, while Eqs. 17 and 18 are consistent with the assumption of a spherical particle and negligible boundary layer concentration gradient. Solution of these equations, with the dimensionless temperature being independent of η (c.f. assumption 2), gives the surface concentration gradient

$$\left(\frac{dC_{A1}^*}{d\eta}\right)_{\eta=1} = \sqrt{k_1}\tanh\sqrt{k_1} + A_1\sqrt{k_1}\,\mathrm{sech}\sqrt{k_1} - 1 \tag{19}$$

where

$$A_1 = \frac{M_2M_3 - M_1}{L_1 - M_3L_2} \tag{20}$$

$$L_1 = \frac{1}{\eta_c^2}\left[\tanh\sqrt{k_1}\cosh\left(\sqrt{k_1}\eta_c\right) - \sinh\left(\sqrt{k_1}\eta_c\right)\right] + \frac{\sqrt{k_1}}{\eta_c}\left[\cosh\left(\sqrt{k_1}\eta_c\right) - \tanh\sqrt{k_1}\sinh\left(\sqrt{k_1}\eta_c\right)\right] \quad (21)$$

$$M_1 = \operatorname{sech}\sqrt{k_1}\left[\frac{\sqrt{k_1}\sinh\left(\sqrt{k_1}\eta_c\right)}{\eta_c} - \frac{\cosh\left(\sqrt{k_1}\eta_c\right)}{\eta_c^2}\right] \quad (22)$$

$$L_2 = \operatorname{cosech}\left(\sqrt{k_2}\eta_c\right) \cdot \left[\sinh\left(\sqrt{k_1}\eta_c\right) - \tanh\sqrt{k_1}\cosh\left(\sqrt{k_1}\eta_c\right)\right] \quad (23)$$

$$M_2 = \operatorname{cosech}\left(\sqrt{k_2}\eta_c\right)\operatorname{sech}\sqrt{k_1}\cosh\left(\sqrt{k_2}\eta_c\right) \quad (24)$$

$$M_3 = \left[\frac{\sqrt{k_2}\cosh\left(\sqrt{k_2}\eta_c\right)}{\eta_c} - \frac{\sinh\left(\sqrt{k_2}\eta_c\right)}{\eta_c^2}\right]\delta \quad (25)$$

$$K_1 = \phi^2 e^{-\epsilon(1-\theta)/\theta} \quad (26)$$

$$K_2 = K_1/\delta \quad (27)$$

The surface concentration gradient in Eq. 19 is necessary for the energy balance to be discussed subsequently. A further quantity of interest is the concentration of A at $\eta = \eta_c$, which is obtained as

$$C^*_{A1}(\eta_c) = \frac{A_2}{\eta_c}\sinh\left(\sqrt{k_2}\eta_c\right) \quad (28)$$

where

$$A_2 = A_1 L_2 + M_2 \quad (29)$$

This concentration is required to establish the equilibrium conditions at η_c. For this purpose it is also necessary to know the concentration of B at η_c and this is solved for by the flux balance

$$\frac{dC^*_{B1}}{d\eta} = -a\frac{dC^*_{A1}}{d\eta}, \quad \eta_c < \eta \le 1 \quad (30)$$

$$C^*_{B1}(1) = 0 \quad (31)$$

in the outer region. Equations 17, 30, and 31 combine to give

$$C^*_{B1}(\eta_c) = a[1 - C^*_{A1}(\eta_c)] \quad (32)$$

For diffusion of A and B in their mixtures $a = 1$ and for simplicity this will be assumed in this study.

Heat transfer

Consistent with past experimental and theoretical evidence we have assumed that heat transfer is controlled by external temperature gradients, so that the pellet is at a uniform temperature. The energy balance may then be written as

$$\theta - 1 = \psi\left(\frac{dC^*_{A1}}{d\eta}\right)_{\eta=1} \quad (33)$$

which must be solved in conjunction with Eqs. 19–27 to obtain the pellet temperature θ. However, before this can be done it is necessary to establish the equilibrium conditions holding at η_c. This is done below.

Vapor-liquid equilibrium

At the position η_c the liquid in the micropores must be in equilibrium with the surrounding vapor in the macropores, for this is where the transition from liquid-filled to vapor-filled micropores takes place. Accordingly, since a hemispherical meniscus must be present at the micropore-macropore intersections, Eq. 10 must be satisfied. In using this equation, however, we make the simplifications that the pure-component vapors are ideal gases, and the gas and liquid mixtures are ideal, so that ϕ_i^{sat}, γ_i, and $\hat{\phi}_i$ are all unity. Further, upon neglecting the effect of the small difference in pressures on the liquid-phase fugacities, we obtain the condition

$$\sum_{i=1}^{N}\frac{y_i P}{p_i^o}\exp\left(2\sigma\cos\hat{\theta}v_i/rR_gT\right) = 1 \quad (34)$$

which must be satisfied at $\eta = \eta_c$. Here N is the number of components. For simplicity we assume that the liquid phase contains mostly A and B, and that the vapor pressure of all other components and inerts, including hydrogen, is much larger than P. Under these conditions Eq. 34 can be rewritten as

$$\left[\frac{C^*_{A1}(\eta_c)}{P^{o*}_A(\theta)} + \frac{C^*_{B1}(\eta_c)}{P^{o*}_B(\theta)}\right]\theta\exp\left(2\sigma\cos\hat{\theta}v/rR_gT_o\theta\right) = 1 \quad (35)$$

in which we have, for convenience, assumed that A and B have the same molar volume v. Setting $\alpha = 2\sigma\cos\hat{\theta}v/rR_gT_o$, and combining with Eq. 32 gives

$$\left\{\frac{C^*_{A1}(\eta_c)}{P^{o*}_A(\theta)} + \frac{a[1 - C^*_{A1}(\eta_c)]}{P^{o*}_B(\theta)}\right\}\theta e^{\alpha(\theta)/\theta} = 1 \quad (36)$$

where α may be a function of θ because of the dependency of the surface tension σ on temperature. The much weaker dependency of the molar volume v on temperature is considered insignificant. In addition the mixture surface tension σ may depend on the liquid-phase composition, but we neglect this effect and assume it to be a function only of temperature over the narrow range of conditions for the steady states that may emerge.

Equations 19–29, 32, 33, and 36 form the model of partial internal wetting of an externally dry catalyst pellet that is to be investigated here. Before these equations can be solved, however, it is necessary to prescribe the functional forms of $\alpha(\theta)$ and $P^{o*}_A(\theta)$, $P^{o*}_B(\theta)$. For the former we assume that the surface tension is linearly dependent on temperature for the narrow range of conditions to be encountered (Reid et al., 1977), so that

$$\alpha(\theta) = f + g\theta \quad (37)$$

where f and g are constants. For the dimensionless vapor pressures we assume the validity of the Clausius-Clapeyron relationship and set

$$P^{o*}_A = P^*_{Ao}\exp\left[-\Delta H^*_A(1 - \theta)/\theta\right] \quad (38)$$

$$P_B^{o*} = P_{Bo}^* \exp\left[-\Delta H_B^*(1-\theta)/\theta\right] \quad (39)$$

where $P_{Ao}^*[=P_A^o(T_o)/C_{Ao}R_gT_o]$ and $P_{Bo}^*[=P_B^o(T_o)/C_{Ao}R_gT_o]$ are the dimensionless vapor pressures of A and B, respectively, at the ambient temperature T_o.

Results and Discussion

Procedure

Equations 19 to 27, 32, 33, and 36 to 39 form a system of nonlinear algebraic equations which must be solved, for given values of the parameters, to obtain the unknowns θ and η_c. The parameters for the problem as formulated are ϕ, δ, ϵ, a, ψ, f, g, P_{Ao}^*, P_{Bo}^*, ΔH_A^*, and ΔH_B^*, all of which are directly or indirectly measurable, or can be estimated from theoretical considerations. Among these, the parameter a is to be taken as unity as discussed earlier. Further, the parameters, δ, ϕ, and ψ are not known *a priori*, but are related to the ratio β according to the conditions of the particular steady state. Here β is the ratio of the effective diffusivity of gaseous A when both micropores and macropores are open, to that when only the macropores are open for diffusion. If at the prevailing steady state temperature $P_A^{o*} > P_B^{o*}$, as calculated from Eqs. 38 and 39, then the micropores in the inner region $0 \le \eta \le \eta_c$ are liquid-filled. Thus, D_{eA1} corresponds to the case of diffusion when all micropores are also available, and D_{eA2} corresponds to the case of diffusion in only the macrostructure. If we maintain as independent parameters the Thiele modulus ϕ_L, and also ψ_L, based on effective diffusivities with only the macrostructure open, we must have

$$\text{for} \quad P_A^{o*}(\theta) > P_B^{o*}(\theta) \quad (40)$$

$$\delta = 1/\beta \quad (41)$$

$$\phi = \phi_L/\sqrt{\beta} \quad (42)$$

$$\psi = \beta\psi_L \quad (43)$$

If instead, at the temperature θ of the steady state, $P_A^{o*} < P_B^{o*}$ micropores in only the outer shell $\eta_c \le \eta \le 1$ are liquid-filled, while those in the interior are vapor-filled. Consequently, we must have

$$\text{for} \quad P_A^{o*}(\theta) < P_B^{o*}(\theta) \quad (44)$$

$$\delta = \beta \quad (45)$$

$$\phi = \phi_L \quad (46)$$

$$\psi = \psi_L \quad (47)$$

Thus, we have replaced the parameters δ, ϕ, and ψ by the parameters β, ϕ_L, and ψ_L, which are all known *a priori*. Also, the equations to be solved simultaneously are now Eqs. 19 to 27, 32, 33, and 36 to 47.

Table 1 lists the values of the parameters that remained unchanged for most of the computations. Since the parameters ϕ_L, ψ_L, and ϵ were varied, their values are specified later. At first a Newton-Raphson procedure, using the variables η_c and θ as unknowns to be solved for, was tried but was unsuccessful. Independent backward calculations showed that the steady states sought did exist, but only over a very narrow range of values of ψ_L for a given ϕ_L and ϵ. Consequently, an alternative procedure was devised in which the independent parameter ψ_L was replaced by η_c. This was much more successful since the range of values of η_c is known $(0 < \eta_c < 1)$. Under this modification Eqs. 19–29, 32, 36–39, 40–42 and 44–46 were first solved simultaneously, using the Newton-Raphson method, and the values of θ, $(dC_{A1}^*/d\eta)_{\eta=1}$ obtained. These were then substituted into Eq. 33 to obtain the value of ψ required to achieve that steady state. Equation 43 or 47, whichever is applicable, then determines the corresponding ψ_L.

Table 1. Parameter Values Used in Computations

Parameter	Value
β	1.5
a	1.0
f	0.725
g	−0.48
P_{Ao}^*	1.0
P_{Bo}^*	0.95
ΔH_A^*	8.0
ΔH_B^*	8.0
ϕ_L	*
ψ_L	*
ϵ	*

*Values specified in figures.

Position of interface

Figure 1, for which $\epsilon = 45$, shows that the steady states sought do indeed exist, albeit over a very narrow range of values of ψ_L for a given value of ϕ_L. For $\phi_L = 4$, for example, a partial micropore wetting steady state exists only for ψ_L in the range of about 3.95×10^{-3} to 4.6×10^{-3}, as seen in Figure 1a, for over this range there is an equilibrium interface η_c in $0 < \eta_c < 1$. Similar narrow ranges for values of ψ_L for which a solution exists were also found for other values of ϕ_L of 0.5, 2, and 5, as evidenced in Figures 1a and b. An interesting feature of these figures is that for $\phi_L = 4$ and $\phi_L = 5$ multiplicity in the position of the equilibrium interface exists for certain ranges of ψ_L values. This is more

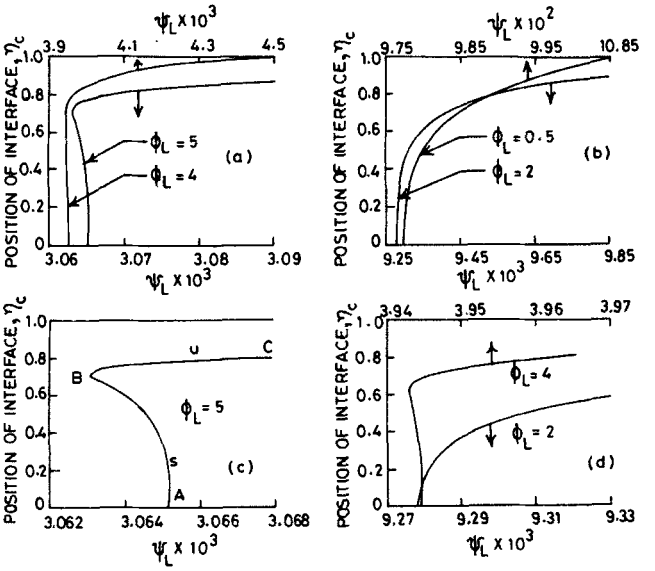

Figure 1. Position of equilibrium interface η_c as a function of ψ_L for various values of ϕ_L.

$\epsilon = 45$; other parameters as in Table 1

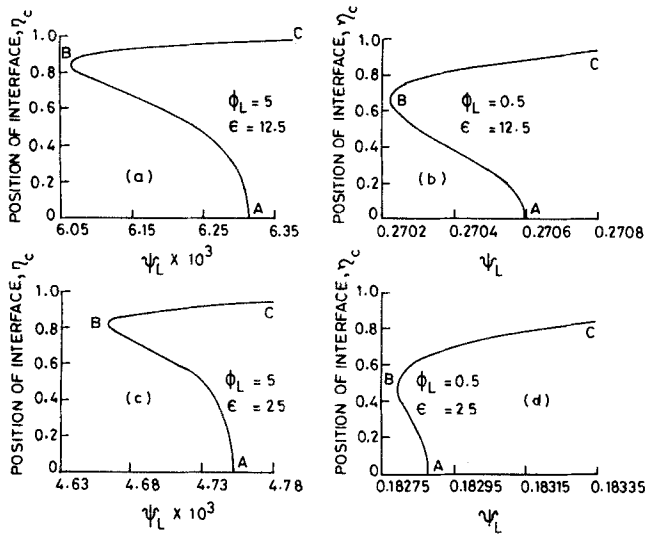

Figure 2. Position of equilibrium interface η_c as a function of ψ_L for various values of ϕ_L and ϵ.
Other parameters as in Table 1

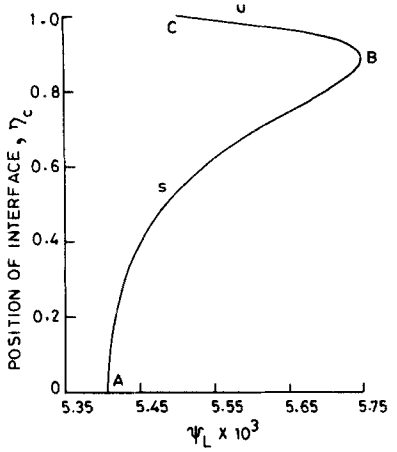

Figure 3. Position of equilibrium interface as a function of ψ_L for $\phi_L = 5$, $\epsilon = 12.5$, $P^*_{Bo} = 1.05$.
Other parameters as in Table 1

clearly brought out in Figures 1c and 1d, where the region of multiplicity has been magnified. As seen in the latter figure, for $\phi_L = 2$ there is no multiplicity, while for $\phi_L = 4$ the multiplicity range for ψ_L is a very small fraction of the range for which there is an interface η_c in $0 < \eta_c < 1$. Thus, it is clear that for a given value of ϵ there is a critical value of the Thiele modulus ϕ_L for which multiplicity in the position of the equilibrium interface can occur.

Similar behavior is also observed at other values of ϵ as shown in Figure 2. For both values of ϵ chosen for the figure, i.e., $\epsilon = 12.5$ and 25, multiplicity occurs even at ϕ_L as low as 0.5, although for $\epsilon = 25$ the region of multiplicity is very narrow. This indicates that the critical value of the Thiele modulus above which multiplicity can occur decreases with decrease in ϵ. Thus, for the smaller values of ϵ the region of multiplicity for ϕ_L is larger.

For the conditions of Figures 1 and 2 $P^{o*}_A > P^{o*}_B$ since $P^*_{Ao} > P^*_{Bo}$ and $\Delta H^*_A = \Delta H^*_B$. Consequently micropores in the inner core $0 \le \eta \le \eta_c$ are liquid-filled and those in the region $\eta_c < \eta \le 1$ are vapor-filled. The situation is reversed however if P^*_{Bo} is increased to 1.05, for now $P^{o*}_A < P^{o*}_B$ and micropores in the outer shell $\eta_c \le \eta \le 1$ are liquid-filled. Figure 3 shows the results for this value of P^*_{Bo}, for $\phi_L = 5$ and $\epsilon = 12.5$. The behavior is similar to that in Figure 2 showing the region of multiplicity. However, in this case with increase in ψ_L the interface moves out from the center on the lower branch, and inward from the outer surface on the upper branch. This behavior is reversed for the lower value of P^*_{Bo} of 0.95 as seen in Figures 1 and 2. This difference in the behavior also has considerable significance regarding stabilities of the different branches, as discussed in a later section.

Figure 4 gives the region of existence of the partial micropore wetting steady states in terms of ϕ_L and ψ_L for the different values of ϵ, with the other parameters as shown in Table 1. The narrow range of values of ψ_L (or ϕ_L) for given ϕ_L (or ψ_L) and ϵ for the steady state is clear from the figure. With decrease in activation energy, and hence ϵ, the region of existence becomes narrower, while with increase in ϕ_L a relatively wider range for ψ_L is found. Thus, there is greater chance of observing these steady states for reactions with a large activation energy, and for conditions of high Thiele modulus. The values of ψ_L required for these steady states are well within the range of typical values of this parameter that are obtained from the data compiled by Froment and Bischoff (1979), so that these states can indeed exist in externally dry pellets in trickle beds. The narrow range of parameter values over which these states exist, however, make them extremely difficult to realize in experiments. Perhaps this is why such partial wetting steady states have been reported only by Kim and Kim (1981a). Consistent with the present conclusion that the possibility of being able to observe these steady states is better at large ϕ_L, Kim and Kim operated at a Thiele modulus of about 10.

It should be noted that the narrow range of parameters reported here has been obtained for an irreversible reaction with

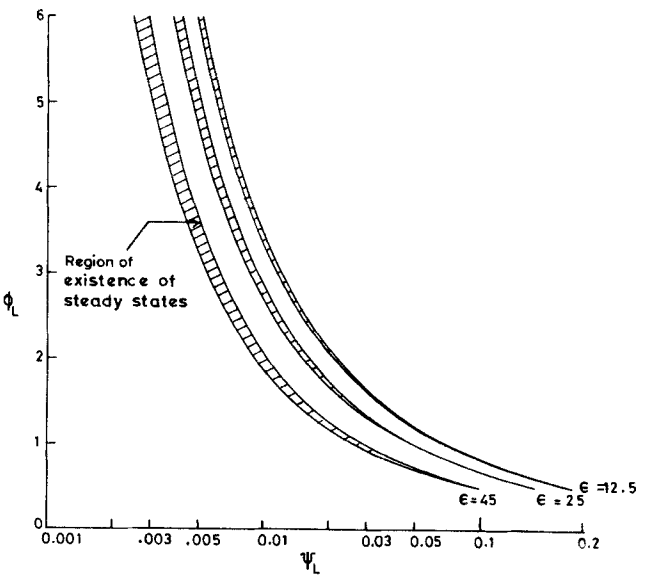

Figure 4. Region of values of ϕ_L and ψ_L at various values of ϵ, for which steady states with partial wetting of micropores exist.
Other parameters as in Table 1

first-order kinetics. For more complex reactions and nonlinear kinetics such as in hydrogenations the behavior may be different, and the band for ψ_L larger or possibly even smaller. The effect of reaction kinetics on these steady states is therefore an aspect that needs further investigation.

Effectiveness factor

Having identified the existence of intermediate steady states with partial wetting of the micropores, it is of interest to study the reaction rates for these states and to compare them with those for complete wetting, and no wetting, of the micropores. To this end we consider the effectiveness factor

$$E = \frac{3(\theta - 1)}{\psi\phi^2} \tag{48}$$

which, as usual, is the ratio of the rate of reaction for the steady state to that which would have been obtained if the entire pore structure was exposed to vapor at the ambient temperature and concentration. In terms of the independent variables ϕ_L and ψ_L Eq. 48 is written as

$$E = \frac{3(\theta - 1)}{\psi_L \phi_L^2} \tag{49}$$

and the dependence of the effectiveness factor on ϕ_L and ψ_L shown in Figures 5–8. In these figures the effectiveness factor curves labeled 2 are those corresponding to the steady states of Figures 1–3. Also superimposed on Figures 5–8 are the effectiveness factor curves corresponding to complete wetting of micropores (curve 3) and no wetting of micropores (curve 1). For the latter case the values of ϕ and ψ were appropriately taken through Eqs. 42 and 43 although the results are plotted in terms of the values of ψ_L and ϕ_L to keep a common basis. It may be noted that for complete or no wetting of the micropores multiplicity also may exist due to thermal and diffusional effects alone, in accordance with the classical analysis of Weisz and Hicks (1962). We have however plotted only the lowest of these steady states, since the others involve excessively high temperatures, or are unstable.

Curve *EDC* in Figure 5 corresponds to curve *BC* in Figure 1c, and is seen to have a lower effectiveness factor than branch *FE*, which corresponds to *AB* of Figure 1c. Curve *GH*, which represents the case of no internal wetting, bifurcates into branches *FH* and *FE* at *F*. Thus, for values of ψ_L between those corresponding to *E* and *F* as many as four steady states are shown in the figure. The fifth, for complete internal wetting, is not considered here and should have a much lower effectiveness factor. For ψ_L between that corresponding to *F* and *G* only one partial micropore wetting steady state exists, along with those for complete micropore wetting and no wetting. Beyond *G* the completely dry state shown ceases to exist (only the higher reactivity ones not considered here do). Also, at *C* the complete micropore wetting state shown as curve 3 ceases to exist. The nonexistence of the complete micropore-filling steady state is confirmed from the fact that for values of ψ_L larger than that corresponding to *C* the quantity $M_L(1)$ obtained from

$$M_L(\eta) = \left[\frac{C_A^*(\eta)}{P_A^{o*}(\theta)} + \frac{a[1 - C_A^*(\eta)]}{P_B^{o*}(\theta)}\right]\theta\, e^{\alpha(\theta)/\theta} \tag{50}$$

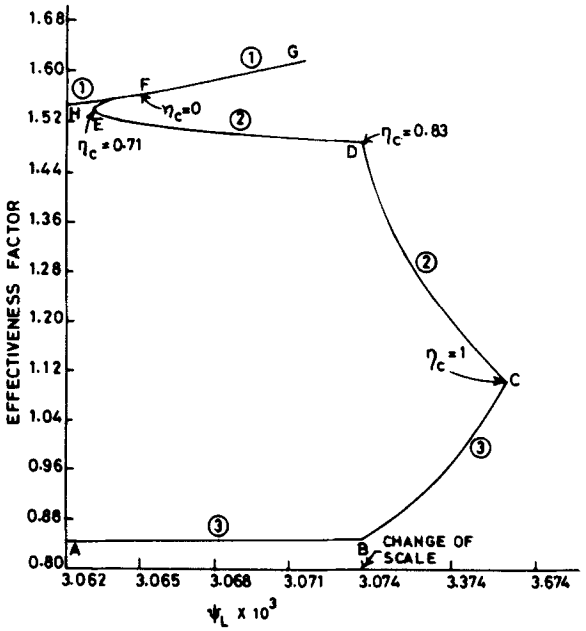

Figure 5. Steady state effectiveness factor as a function of ψ_L for ϕ_L = 5 and ϵ = 45.
Other parameters as in Table 1

is less than unity, suggesting evaporation at the particle surface.

As seen in Figure 5 there is substantial difference among the effectiveness factors of the completely dry and complete micropore wetting states, with the partial micropore wetting states spanning the range between the two. On reducing the value of ϕ_L into the region in which only one partial micropore wetting state occurs, however, the curve for completely dry operation no longer shows a bifurcation as shown in Figures 6a and 6b. Indeed, the state of partial micropore wetting can even have a higher effectiveness than the completely dry state. On reducing the value of ϕ_L to 0.5, as shown in Figure 6b, the complete micropore filling state also no longer meets the partial micropore filling state. In addition, the latter state has an effective factor more than twice that of even the completely dry state. However, as will be subsequently shown this state is likely to be unstable. A further feature in Figure 6b is that for values of ψ_L below about 0.099 (corresponding to point *B*) the completely dry state

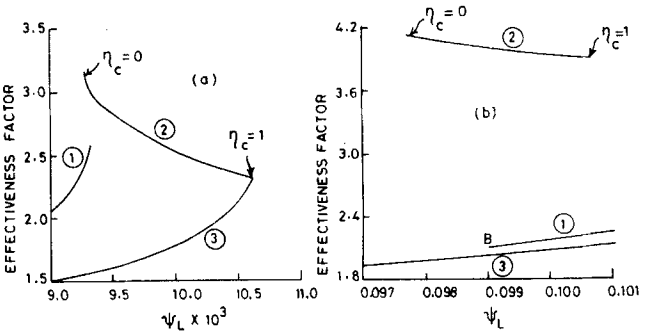

Figure 6. Steady state effectiveness factor as a function of ψ_L for ϵ = 45.
a. ϕ_L = 2; b. ϕ_L = 0.5.
Other parameters as in Table 1

is no longer stable as condensation takes place in the micropores at the center. This is confirmed from the fact that $M_v(0)$ obtained from

$$M_v(\eta) = \left\{ \frac{C_A^*(\eta)}{P_A^{o*}(\theta)} + \frac{a[1 - C_A^*(\eta)]}{P_B^{o*}(\theta)} \right\} \theta \, e^{\alpha'(\theta)/\theta} \qquad (51)$$

where

$$\alpha'(\theta) = \alpha(\theta)/2 \cos \hat{\theta} \qquad (52)$$

becomes greater than unity, suggesting condensation. Here $\alpha'(\theta)$ is defined by Eq. 52 in accordance with Eq. 12 for condensation. In addition, the wetting angle $\hat{\theta}$ is taken as 0° for simplicity. The same value is chosen by Gregg and Sing (1981) in their presentation of the subject.

For the values of ϵ of 12.5 and 25, for which multiple partial micropore filling states were found in Figure 2, the behavior for $\phi_L = 0.5$ and $\phi_L = 5$ is similar to that shown in Figure 5. Figure 7 details the variation of the effectiveness factor for these cases. As is to be expected, the effectiveness factor variation is small for $\phi_L = 0.5$, for under these conditions the effect of the effective diffusivity difference between the partial wetting and no wetting states is reduced.

For the cases shown in Figures 5–7 the value of P_{Bo}^* is set at 0.95. Figure 8 shows the effectiveness factor plot corresponding to Figure 3, for which $P_{Bo}^* = 1.05$ and $\epsilon = 12.5$, $\phi_L = 5$. In this case an outer shell is liquid-filled for the partial wetting states. Here also, the curve for no wetting (curve 1) bifurcates as shown at point C. On the other hand curve 3 for complete micropore filling is continuous at point A, at which point evaporation at the center just begins.

Stability

Having established the existence of the multiple steady states with partial micropore wetting, it is of interest to study also the stability of these states. A rigorous analysis of the stability is however possible only by means of a transient model of the system (Aris, 1975), and is not attempted in this study. However, a preliminary analysis may be done using the classical Van Heerden (1953) approach which, while developed for autothermic reactors, has been found useful also for gas-solid systems (Shen and Smith, 1965; Ishida and Wen, 1968; Beveridge and Goldie, 1968; Wen and Wang, 1970). The technique is based on steady state analysis alone and, as discussed by Froment and Bischoff (1979) with reference to the stirred-tank reactor, it provides only a necessary but not sufficient condition for stability. The analogy between the equations for catalyst particles and stirred tanks has been lucidly developed by Aris (1975), and provides support for the use of the Van-Heerden approach here. It may be mentioned that even with transient modeling, if the gas concentration is taken to be at the pseudosteady state and the temperature gradient is confined to the boundary layer as in McGreavy and Thornton (1970), the results become similar to those obtained by the steady state approach.

To investigate the stability we examine a curve such as that in Figure 1c showing two partial wetting states over a range of values of ψ_L. From its definition it is clear that ψ_L is representative of the ratio of rate of heat generation to rate of heat loss. Now consider a steady state on the segment AB. If there were a small

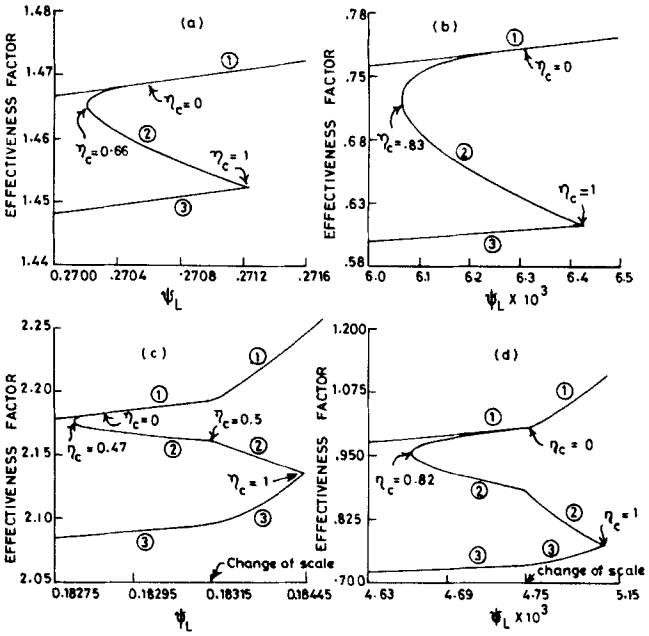

Figure 7. Effectiveness factor as a function of ψ_L.
a. $\epsilon = 12.5$, $\phi_L = 0.5$; b. $\epsilon = 12.5$, $\phi_L = 5$
c. $\epsilon = 25$, $\phi_L = 0.5$; d. $\epsilon = 25$, $\phi_L = 5$
Other parameters as in Table 1

positive perturbation in temperature the equilibrium interface would move inward to a smaller value of η_c. The new state however requires a higher value of ψ_L, which implies a higher rate of heat generation relative to heat loss, than the actual value. As a result the system will cool down to its original state. Similarly, for small negative perturbations also it is easily seen that the system will return to its original state. Thus the curve AB meets the necessary criterion for stability. However, by the same analysis segment BC is found to be unstable, for any temperature perturbation tends to move the system away from its original state.

It is clear from the above that the unique steady states of partial micropore wetting in Figure 1b for $\phi_L = 0.5$ and 2 are unstable. Similarly, in Figures 2 and 3 for each curve the lower segment AB satisfies the necessary condition for stability while the

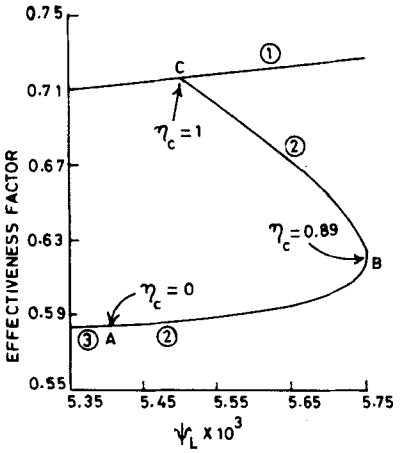

Figure 8. Effectiveness factor as a function of ψ_L for $\epsilon = 12.5$, $\phi_L = 5$, $P_{BO}^* = 1.05$.
Other parameters as in Table 1

upper segment BC does not and is likely to be unstable. Thus, the high effectiveness factor curves in Figure 6 correspond to unstable, although unique, partial micropore wetting steady states.

The above observations may also be quantified by considering the curves of dimensionless heat generation and heat loss defined by

$$Q_G = \left(\frac{dC^*_{A1}}{d\eta}\right)_{\eta=1} \tag{53}$$

$$Q_L = \frac{\theta - 1}{\psi} \tag{54}$$

in accordance with Eq. 33. Figure 9 shows the heat generation curve plotted as βQ_G vs. θ for $\epsilon = 25$ and $\phi_L = 5$, corresponding to the states in Figure 2c. For the heat loss line AD, representing βQ_L for which $\psi_L = 4.73 \times 10^{-3}$, there are two intersections, B and C, with the curve for heat generation, consistent with Figure 2c. At the upper steady state, at point C

$$\frac{dQ_G}{d\theta} < \frac{dQ_L}{d\theta} \tag{55}$$

satisfying the necessary condition for stability (Froment and Bischoff, 1979). However, at the lower steady state B

$$\frac{dQ_G}{d\theta} > \frac{dQ_L}{d\theta} \tag{56}$$

showing the state to be unstable. From the values of η_c noted alongside the curve for heat generation it is clear that the lower segment AB in Figure 2c can be stable while the upper segment BC is unstable. This is in agreement with the qualitative discussion of the above paragraph. A further point to be noted in Figure 9 is that in the region of a single intermediate steady state such as for $\psi_L = 4.78 \times 10^{-3}$, instability occurs.

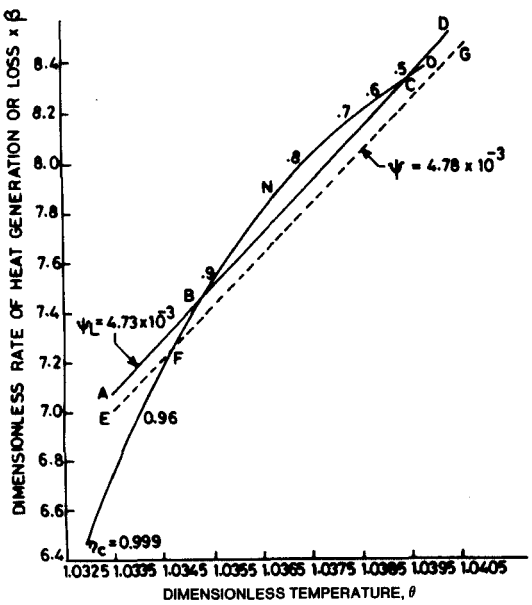

Figure 9. Heat generation and heat loss curves for $\epsilon = 25$ and $\phi_L = 5$.
Other parameters as in Table 1

Conclusions

In this work it has been shown that over a narrow range of parameter values, even for a first-order reaction in a catalyst pellet exposed to saturated vapor, steady states can exist in which micropores in an inner core or an outer shell are liquid-filled. Under certain conditions even two such steady states can exist. When only one such steady state exists then it is found to be unstable. When two such steady states exist only one of them can be stable, while the other is shown to be unstable.

The effect of lack of thermodynamic equilibrium in the liquid-filled region has not been investigated here and is an open problem for future study. Further, for systems with nonlinear kinetics, or those having a larger difference in vapor pressure between reactant and product, the behavior is likely to be more complex and needs to be studied.

Notation

$a = D_{eA1}/D_{eB1}$
$\hat{a}_i$ = activity of component i
A = frequency factor
A_1 = Eq. 20
A_2 = Eq. 29
C_{Ao} = ambient concentration of A
C_{A1} = local vapor phase concentration of A in the region $\eta_c \le \eta \le 1$
C_{A2} = local vapor phase concentration of A in the region $0 \le \eta \le \eta_c$
$C^*_{A1} = C_{A1}/C_{Ao}$
$C^*_{A2} = C_{A2}/C_{Ao}$
C_{B1} = local vapor phase concentration of B in the region $\eta_c \le \eta \le 1$
$C^*_{B1} = C_{B1}/C_{Ao}$
D_{eA1} = vapor phase effective diffusion coefficient of A in $\eta_c < \eta \le 1$
D_{eA2} = vapor phase effective diffusion coefficient of A in $0 \le \eta \le \eta$
D_{eAL} = vapor phase effective diffusion coefficient of A when micropores are liquid-filled and only macropores are open
D_{eAv} = vapor phase effectivity diffusivity of A when all pores are open
D_{eB1} = vapor phase effective diffusivity of B in $\eta_c < \eta \le 1$
E = effectiveness factor
E_R = activation energy
f = Eq. 37
f_i^l = liquid phase fugacity of pure component i
f_i^{sat} = fugacity of pure component i at saturation
$\hat{f}_i^l$ = mixture fugacity of component i in liquid phase
$\hat{f}_i^v$ = mixture fugacity of component i in vapor phase
g = Eq. 37
G = Gibbs free energy
$\bar{G}_i$ = partial molar Gibbs free energy of component i
G_i^o = standard state Gibbs free energy of component i
$\bar{G}_i^l$ = partial molar Gibbs free energy of component i in liquid phase
$\bar{G}_i^v$ = partial molar Gibbs free energy of component i in vapor phase
ΔG^o = standard Gibbs free energy change
h = external heat transfer coefficient
ΔH_A = enthalpy of vaporization of pure A
$\Delta H^*_A = \Delta H_A/RT_o$
ΔH_B = enthalpy of vaporization of pure B
$\Delta H^*_B = \Delta H_B/RT_o$
ΔH_R = heat of reaction
k_{so} = reaction rate constant at temperature $T_o = Ae^{-E_R/R_gT_o}$
K_1 = Eq. 26
K_2 = Eq. 27
l = length
L_1 = Eq. 21
L_2 = Eq. 23
M_1 = Eq. 22
M_2 = Eq. 24
M_3 = Eq. 25
M_L = Eq. 50
M_V = Eq. 51

n_i = number of moles of component i
N = total number of components
P = pressure
P_A^o = saturation vapor pressure of A on a flat surface
P_A^{o*} = dimensionless saturation vapor pressure, Eq. 38
$P_{Ao}^* = P_A^o(T_o)/C_{Ao}R_gT_o$
P_B^o = saturation vapor pressure of B on a flat surface
P_B^{o*} = Eq. 39
$P_{Bo}^* = P_B^o(T_o)/C_{Ao}R_gT_o$
P_i^o = saturation vapor pressure on a flat surface
Q_G = dimensionless rate of heat generation, Eq. 53
Q_L = dimensionless rate of heat loss, Eq. 54
r = micropore radius
r_M = macropore radius
R = radial position in pellet
R_g = gas constant
R_o = pellet radius
R_c = position of equilibrium interface
S_o = surface area per unit volume
T = temperature
T_o = ambient temperature
v = molar volume
$\bar{v}_i$ = partial molar volume of component i
$\underline{v}_i$ = pure component molar volume of component i
$\Delta\bar{v}$ = Eq. 6
X_i = mole fraction of i in liquid phase
y_i = mole fraction of i in vapor phase

Greek letters

$\alpha = 2\sigma \cos\hat{\theta} v/r R_gT_o$
$\alpha' = \alpha/2\cos\theta$
$\beta = D_{eAv}/D_{eAL}$
$\delta = D_{eA2}/D_{eA1}$
$\eta = R/R_o$
$\eta_c = R_c/R_o$
ϵ_i = stoichiometric coefficient of i
$\epsilon = E_R/R_gT_o$
γ_i = activity coefficient
$\phi = R_o\sqrt{k_{so}S_o/D_{eA1}}$
$\hat{\phi}_i$ = fugacity coefficient of i in mixture
$\hat{\phi}_i^{sat}$ = fugacity coefficient of pure i at saturation
$\phi_L = R_o\sqrt{k_vS_o/D_{eAL}}$
$\psi = D_{eA1}C_{Ao}(-\Delta H_R)/hR_oT_o$
$\psi_L = D_{eAL}C_{Ao}(-\Delta H_R)/hR_oT_o$
σ = surface tension
$\theta = T/T_o$
$\hat{\theta}$ = contact angle
ζ = extent

Appendix: Criterion for No Wetting of Macropores

For a given steady state it is possible to estimate the validity of the assumption of no macropore filling by liquid. Here, we recognize that since locally the micropores are liquid-filled, a vapor-liquid interface exists, and by capillary transport the macropores can be filled even under conditions in which Eq. 12, the generalized Cohan equation, predicts no condensation. Consequently Eq. 10 or its simplified dimensionless form Eq. 35 applies for determining the condition of no wetting of macropores, which may be written as

$$\left\{\frac{C_A^*(0)}{P_A^{o*}(\theta)} + \frac{a[1 - C_{A1}^*(0)]}{P_B^{o*}(\theta)}\right\}\theta \cdot \exp(2\sigma\cos\hat{\theta}v/r_MR_gT_o\theta) < 1 \quad \text{(A1)}$$

for $P_A^{o*}(\theta) > P_B^{o*}(\theta)$, since for this case condensation will occur in an inner core. Similarly, for $P_A^{o*}(\theta) < P_B^{o*}(\theta)$

$$\left\{\frac{C_A^*(1)}{P_A^{o*}(\theta)} + \frac{a[1 - C_{A1}^*(1)]}{P_B^{o*}(\theta)}\right\}\theta \cdot \exp(2\sigma\cos\hat{\theta}v/r_MR_gT_o\theta) < 1 \quad \text{(A2)}$$

since in this case condensation occurs in an outer shell. Here θ is the dimensionless temperature of the steady state and r_M the radius of the smallest macropore. As a point of interest we take the case of $P_A^{o*}(\theta) < P_B^{o*}(\theta)$, and assume $a = 1$, $\sigma\cos\hat{\theta} = 0.01$ J/m^2, $v = 0.1$ m^3/kmol, $T_o = 500$ K, $P_{Ao}^* = 1$, $\Delta H_A^* = 8$. For a steady state for which $\theta = 1.035$ these data may be used in Eqs. 38 and A2 to yield $r_M > 20$ Å. Macropores are always larger than 40 Å in diameter, and numerous catalysts have micropores smaller than this size. Thus, steady states with liquid-filling of micropores but not of macropores are indeed possible in trickle-bed reactor operation.

Literature Cited

Aris, R., *The Mathematical Theory of Diffusion and Reaction in Permeable Catalysts, 2: Questions of Uniqueness, Stability and Transient Behaviour,* Oxford, Bristol (1975).

Beveridge, G. S. G., and P. J. Goldie, "Effectiveness Factors and Instability in Noncatalytic Gas-Solid Reactions: The Effect of Solid Heat Capacity," *Chem. Eng. Sci.*, **23,** 913 (1968).

Cohan, L. H., "Sorption Hysteresis and the Vapor Pressure of Concave Surfaces," *J. Am. Chem. Soc.*, **60,** 433 (1938).

Colombo, A. J., G. Baldi, and S. Sicardi, "Solid-Liquid Contacting Effectiveness in Trickle-Bed Reactors," *Chem. Eng. Sci.*, **31,** 1101 (1976).

Defay, R., and I. Prigogine, *Surface Tension and Adsorption,* Longmans, London (1966).

Drobyshevich, V. I., V. A. Kirillov, and N. A. Kuzin, "A Mathematical Model of the Process with Phase Transition on the Porous Catalyst Pellet," *Chem. Eng. Commun.*, **22,** 151 (1983).

Everett, D. H., "Thermodynamics of Multiphase Fluids in Porous Media," *J. Colloid Inter. Sci.*, **52,** 189 (1975).

Froment, G. F., and K. B. Bischoff, *Chemical Reactor Analysis and Design,* Wiley, New York (1979).

Gregg, S. J., and K. S. W. Sing, *Adsorption, Surface Area and Porosity,* Academic Press, London (1982).

Hanika, J., K. Sporka, V. Ruzicka, and J. Hrstka, "Measurement of Axial Temperature Profiles in an Adiabatic Trickle-Bed Reactor," *Chem. Eng. J.*, **12,** 193 (1976).

Herskowitz, M., "Wetting Efficiency in Trickle-Bed Reactors. The Overall Effectiveness Factor of Partially Wetted Catalyst Particles," *Chem. Eng. Sci.*, **36,** 1665 (1981a).

———, "Wetting Efficiency in Trickle-Bed Reactors: Its Effect on Reactor Performance," *Chem. Eng. J.*, **22,** 167 (1981b).

Herskowitz, M., R. G. Carbonell, and J. M. Smith, "Effectiveness Factors and Mass Transfer in Trickle-Bed Reactors," *AIChE J.*, **25,** 272 (1979).

Hu, R., and T. C. Ho, "Steady State Multiplicity in an Incompletely Wetted Catalyst Particle," *Chem. Eng. Sci.*, **42,** 1239 (1987).

Ishida, M., and C. Y. Wen, "Effectiveness Factors and Instability in Solid-Gas Reactions," *Chem. Eng. Sci.*, **23,** 125 (1968).

Kim, D. Y., and Y. G. Kim, "An Experimental Study of Multiple Steady States in a Porous Catalyst Due to Phase Transition," *J. Chem. Eng. Japan,* **14,** 311 (1981a).

———, "Simulation of Multiple Steady States in a Porous Catalyst Due to Phase Transition," *J. Chem. Eng. Japan,* **14,** 318 (1981b).

McGreavy, C., and J. M. Thornton, "Stability Studies of Single Catalyst Particles," *Chem. Eng. J.*, **1,** 296 (1970).

Mills, P. L., and M. P. Dudukovic, "Application of the Method of Weighted Residuals to Mixed Boundary Value Problems: Dual-Series Relations," *Chem. Eng. Sci.*, **35,** 1557 (1980).

———, "Integral Equation Solution for the Effectiveness Factor of Partially Wetted Catalysts," *Ind. Eng. Chem. Fundam.*, **21,** 90 (1982).

Ramachandran, P. A., and J. M. Smith, "Effectiveness Factors in Trickle-Bed Reactors," *AIChE J.*, **25,** 538 (1979).
Reid, R. C., J. M. Prausnitz, and T. K. Sherwood, *The Properties of Gases and Liquids,* McGraw-Hill, New York (1977).
Sakornwimon, W., and N. D. Sylvester, "Effectiveness Factors for Partially Wetted Catalysts in Trickle-Bed Reactors," *Ind. Eng. Chem. Process Des. Dev.*, **21,** 16 (1982).
Sandler, S. I., *Chemical and Engineering Thermodynamics,* Wiley, New York (1977).
Satterfield, C. N., and F. Ozel, "Direct Solid-Catalyzed Reaction of a Vapor in an Apparently Completely Wetted Trickle-Bed Reactor," *AIChE J.*, **19,** 1259 (1973).
Sedriks, W., and C. N. Kenney, "Partial Wetting in Trickle-Bed Reactors—The Reduction of Crotonaldehyde Over a Palladium Catalyst," *Chem. Eng. Sci.*, **28,** 559 (1973).
Shen, J., and J. M. Smith, "Diffusional Effects in Gas-Solid Reactions," *Ind. Eng. Chem. Fundam.*, **4,** 293 (1965).
Weisz, P. B., and J. S. Hicks, "The Behavior of Porous Catalyst Particles in View of Internal Mass and Heat Diffusion Effects," *Chem. Eng. Sci.*, **17,** 265 (1962).
Wen, C. Y., and S. C. Wang, "Thermal and Diffusional Effects in Solid-Gas Reactions," *Ind. Eng. Chem.*, **62,** 30 (1970).
Van Heerden, C., "Autothermic Processes—Properties and Reactor Design," *Ind. Eng. Chem.*, **45,** 1242 (1953).
Yentekakis, J. V., and C. G. Vayenas, "Effectiveness Factors for Reactions Between Volatile and Nonvolatile Components in Partially Wetted Catalysts," *Chem. Eng. Sci.*, **42,** 1323 (1987).

Manuscript received Oct. 14, 1987, and revision received Jan. 20, 1988.